Supplementary Materials

Supplementary Methods

Cell culture

The MCF7, ZR-75 and T47D BC cell lines were purchased from the ATCC. 4T1 murine BC cells were also purchased from the ATCC. MDA231-4175 (LM2) is a lung metastatic sub-line derived from the MDA231 BC cell line in the Massagué laboratory [1]. The BoM2 bone metastatic sub-line is derived from MCF7 following a similar procedure as described in [2]. These cell lines and their genetically modified derivatives were grown in DMEM or RPMI medium (Gibco) supplemented with 10% fetal bovine serum (FBS) (Biological Industries), Glutamine 0.29 mg/ml (Biological Industries), Penicillin 100 U/ml (Biological Industries) and Streptomycin 0.1 mg/ml (Biological Industries).

Stable cell lines expressing the shRNA MAF or a non-silencing shRNA were generated as described [3]:

MAF #1-

CCGGTGGAAGACTACTACTGGATGACTCGAGTCATCCAGTAGTAGTCTTCCATTTTT

MAF#2-

CCGGATTTGCAGTCATGGAGAACCACTCGAGTGGTTCTCCATGACTGCAAATTTTTT

Control-

CCGGCTGTTGCTATCGGGTCAACAACTCGAGTTGTTGACCCGATAGCAACAGTTTTTG.

PTHLH -

CCGGCGACGATTCTTCCTTCACCATCTCGAGATGGTGAAGGAAGAATCGTCGTTTTTG

For MAF overexpression in cells, cDNA sequences of MAF isoforms were cloned into the retroviral vector pBabePuro. All cell lines were stably transduced with TK-GFP-Luciferase construct and sorted for GFP.

Animal studies and xenografts

All animal work was approved by the institutional animal care and use committee of IRB Barcelona. Female BALB/c nude mice of 11 weeks of age were used for all studies. For

intracardiac and tail vein injections, cells were resuspended in PBS and injected into the left cardiac ventricle or tail vein of mice using a 26G needle as previously described [3]. Prior to injection, mice were anesthetized with ketamine (100 mg/kg body weight) and xylazine (10 mg/kg body weight). Immediately after injection of tumor cells, mice were imaged for luciferase activity. Mice continued to be monitored weekly using IVIS imaging, unless otherwise indicated. For the injection of tumor cells into the orthotopic site, mice were treated as described above, and tumor cells were mixed with Matrigel before inoculation. Upon becoming palpable, tumors were measured with a digital caliper. Tumors were resected when reaching 300 mm^3. In order to block PTHrP activity *in vivo*, animals were administered, twice a day, 6 μg of (7-34Aa) PTHrP antagonist peptide (Bachem, Switzerland) dissolved in PBS. Control groups were treated with PBS. For all mice implanted with ER+ BC cells, estrogen supply was provided by subcutaneous implanted estrogen pellets (90-day release)(Innovative Research of America, USA).

For intra-tibial injections, BALB/c nude mice were anesthetized using a mixture of ketamine (100 mg/kg) and xylazine (10 mg/kg). The injection site was prepped with a betadine scrub followed by a 70% alcohol wipe. A 1-cm skin incision was made on the antero-medial part of the leg, and the muscle was moved using blunt forceps. The bone was drilled using a 26G syringe-needle (BD Syringes). Single-cell suspensions ($2x10^4$ cells) in a final volume of 25 μl were injected into the upper half of the tibia medullary cavity, as felt by a lack of resistance when injecting cells into the cavity. The skin was sutured, and inoculations were confirmed by bioluminscence. Development of bone lesions was followed by weekly BLI imaging.

In order to perform *ex vivo* imaging, animals were injected with luciferin prior to sacrifice and organs of interested tested for metastatic growth by bioluminescence 5 minutes post injection.

Oligonucleotide array assays

RNA sample collection and generation of biotinylated complementary RNA (cRNA) probe were carried out essentially as described in the standard Affymetrix (Santa Clara, CA) GeneChip protocol. Ten micrograms of total RNA was used to prepare a cRNA probe using a

Custom Superscript Kit (Invitrogen). For expression profiling, 25 ng of RNA per sample was processed using isothermal amplification SPIA Biotin System (NuGEN technologies). Each sample was hybridized with an Affymetrix Human Genome U133APlus2.0 microarray at the IRB Barcelona Functional Genomics Core Facility. All microarray statistical analyses were performed using Bioconductor [4]. Background correction, quantile normalization, and RMA summarization was performed as implemented in the Bioconductor Affy package [5]. Biases caused by experimentation date and family relations between mice were removed by ANOVA adjustment. A semi-parametric empirical Bayes [6] procedure based on moderated t-tests [7] as implemented in the limmapackage was performed to select the bone metastasis-enriched genes by setting the Bayesian FDR at 5% [6]. Additionally, only genes with an absolute fold change greater than 2 were considered differentially expressed. CNA and gene expression datasets from the experimental models can be found at GSE51238.

Analysis of copy number alterations in expression data

The detection of CNAs by means of expression profile analysis is based on strong correlation between the genomic alterations and the aberrant gene expression in the affected genomic regions. While the detection of CNAs using gene expression analysis is possible, difficulties arise from the type of starting expression data [8]. We used the function findCopyNumber from the Bioconductor phenoTest package, which implements an approach similar to the one applied by Hu et al. (2009), to find regions with CNAs in the MSKCC/EMC cohort. Enrichment scores (in our case log hazard ratios) and the chromosomal positions of the scores allowed us to distinguish areas in which the enrichment was higher/lower than expected when the positions were assigned at random.

Within each chromosome, a smoothed score for each gene was obtained via generalized additive models, the smoothing parameter for each chromosome being chosen via cross-validation. The smoothing parameter of each chromosome was used in permutations.

We assessed statistical significance by permuting the positions through the whole genome. For each gene, the permutations of genes in an area with a similar density (distance to tenth

gene) were used to compute p-values (p-values were adjusted using the Benjamini and Hochberg method).

CNAs in the highly bone metastatic BoM2 cells were analyzed. We isolated high-molecular weight DNA from MCF7 and BoM2 cells cultured *in vitro* by means of the GeneElute™ Mammalian Genomic DNA Miniprep Kit (Sigma-Aldrich), following the manufacturer's instructions. The quantity and quality of DNA was determined using a NanoDrop ND-1000 UV-Vis Spectrophotometer and electrophoresis in 1% agarose gel. Genetic aberrations were detected using NimbleGen Human CGH 3x720K Whole-Genome Tiling v3.0 Array consisting of 72,000 probes. Samples were independently labeled with the indicated fluorochromes, namely Cy3 for BoM2 and Cy5 for MCF7 reference sample, and co-hybridized. The copy number analysis was performed using Bioconductor. Briefly, log2 fold changes were normalized by a mode normalization and outlier smoothing [9]. Preprocessing, segmentation, post-segmentation, and segment classification were performed as implemented in the Bioconductor CGHcall package. For all chromosomes, dots and blue horizontal lines represent normalized log2 intensity ratios and segments. The probability of copy number gain is indicated by the length of the green downward bar, and loss probability by red upward bar.

From The Cancer Genome Atlas (TCGA) breast cancer project, a total of 773 breast tumours were assayed using Affymetrix 6.0 SNP arrays. Segmentation analysis and GISTIC were used to identify focal amplifications/deletions and arm-level gains and losses. In particular, we evaluated DNA copy-number changes of each gene using Level 3 GISTIC data (high-level amplification, low-level amplification, neutral, low-level deletion and high-level deletion), which is publicly available at the TCGA portal (https://tcga-data.nci.nih.gov/tcga/).

Protein extraction and Western Blot

Cells were lysed with a buffer containing 1% Triton in 50mM Tris/HCl (pH 7.4) for protein extracts and processed as in [3]. The tumor samples were mechanically homogenized in a buffer containing 0.5% NP-40, in 150mM Tris/HCl (pH 7.5) and 150 mM NaCl and processed as stated above. The antibodies used were anti-MAF rabbit polyclonal (AbCam;

dilution 1:500) or rabbit monoclonal (Inbiomotion; dilution 1:50), α-Tubulin mouse monoclonal (Sigma; dilution 1:10000) and b-Actin mouse monoclonal (Sigma; dilution 1:20000).

Chromatin Immunoprecipitation (ChIP)

Indicated cells were grown to 70% confluence and subsequently cross-linked with 1% formaldehyde at room temperature for 15 min. ChIP was performed as described previously [10]. The antibodies used were MAF (Santa Cruz) and anti-acHis4 (Usptate). A 166-bp segment of the distal region of the PTHrP promoter (nucleotides -3406 to -3240) was amplified with the following primers (PR4 set): 5'- GGTGCTCTTGCTGTGTCTC-3' (sense) and 5'- CTTTCCGTAGAAATTCTCCTC-3' (antisense). In the proximal region of the *PTHrP* promoter (nucleotides -425 to -566) two primer sets were used. A 181-bp segment was amplified with the following primers (PR1 set): 5'- GGCTAACCGCCTCCTAAAAG-3' (sense) and 5'-TTGTTCTCAGGGTGTGTGGA-3' (antisense). As a negative control, a 166-bp region of the □-actin promoter (nucleotides 29 to 195) was amplified with the following primers: 5'-TCGAGCCATAAAAGGCAACTT-3' (sense) and 5'-AAACTCTCCCTCCTCCTCTTCC-3' (antisense).

Quantitative real-time PCR

Total RNA was isolated and processed as described [3]. Human *MAF long, CND1, MYC* and *B2M,* the latter as endogenous control, were amplified with commercially designed TaqMan gene expression assays (Applied Biosystems). Expression levels of human *MAF short* were assessed and normalized to beta-actin levels using Syber Green real-time PCR reaction (Applied Biosystem) using the following primers: *MAF short-F*: 5'GATCCACAGCACTGGTCTTG3', *MAF short-R*: 5'GGGATGCTGCTGAGGTTAAA 3', *beta-ACTIN*-F: 5' TCACCCACACTGTGCCCATCTACGA 3', and *beta-ACTIN*-R: 5'CAGCGGAACCGCTCATTGCCAATGG 3'.

Histopathology and immunohistochemistry

Hind limb bones were excised, fixed in 10% neutral-buffered formalin, decalcified, embedded in paraffin, and subjected to staining with hematoxylin and eosin (H&E, Richard-Allan Scientific Inc.), anti-Ki67 mouse monoclonal antibody (Novocastra, dilution 1:500), and tartrate-resistant acid phosphatase (TRAP) (Sigma). Osteoclast number was assessed TRAP-positive cells along the tumor-bone interface on TRAP-stained sections, and expressed as positive cell number per perimeter of interface. Minimum of 10 random fields per metastasis, covering the whole lesion area, were captured. The following variables were measured in bone metastasis: total tumor area, total bone area (B.Ar), total tissue area (Tt.Ar). These variables were reported as Bone Volume (BV/TV or percent of tissue space occupied by bone=100*(B.Ar/Tt.Ar)), Bone area (mm2) and Tumor Area (mm2), nº TRAP+ cells/Tumor Bone interface (cells/mm). Of note, bone trabecular volume (BV/TV) is an estimate of the tissue space occupied by bone and/or tumor tissue but does not consider bone marrow space.

MAF immunostaining was performed using 3-µm human BC tumor sections placed on plus-charged glass slides in a Dako Link platform. After deparaffinization, heat antigen retrieval was performed in 0.01 mol/L citrate-based buffered solution (Dako), pH6.1. Endogenous peroxidase was quenched. A rabbit polyclonal anti-MAF antibody was used for 30 min at room temperature, 1:100 dilution, followed by incubation with an anti-rabbit Ig dextran polymer coupled with peroxidase (Flex+, Dako). Sections were then visualized with 3,3'-diaminobenzidine (DAB) and counterstained with Hematoxylin.

MAF antibody sensitivity (1:100) had been calculated in a range of crescent dilutions of primary antibody from 1:10 to 1:1000. Specificity was determined using parental and MAF-overexpressing (plusMAFlong/short) MCF7 and T47D human BC cells. Formalin-fixed cell pellets were processed as described for IHC, and results confirmed by Western blot from whole lysates. Specificity was also shown in heterotopic MCF7 and MAF-overexpressing MCF7 xeno-implants in BALB/c nude mice. Sections from the same specimens incubated with normal rabbit IgG2 (IS600, Dako) instead primary antibodies were used as negative controls.

MAF immunostaining was scored by a computerized measurement. Nine representative images from each specimen were acquired at 10-nm intervals between 420 and 700 nm, using a DM2000 Leica microscope equipped with the Nuance FX Multispectral Imaging System (CRI Inc). Before acquiring a spectral dataset of an image, an auto-exposure routine was performed while imaging a blank area of slides to determine the exposure time necessary to fill approximately 90% of the wells of the device at each wavelength to compensate for variations in source intensity, filter transmission efficiency, and camera sensitivity. A library of pure DAB and Hematoxylin dye colors was built and used to separate the colors using the Nuance 1.6.4 software. A cube (stack of images taken at the different wavelengths) of reference was then acquired for each new case, followed by spectral imaging of three representative tissue fields using the same exposure times. After deconvolution of the images, the spectral data was flat-fielded to compensate for unevenness in illumination, and background was filtered. The positive signals were converted from transmission to optical density units by taking the negative log of the ratio of the sample divided by the reference cube using a Beer law conversion. A computer-aided threshold was set to create a pseudo-color image that highlights all of the positive signals. Analysis yielded quantitative data of MAF from the average intensity of regions of interest. Only the nuclei of epithelial cells (normal and malignant), but not those of stromal cells or lymphocytes, were automatically detected by setting a distinct size threshold and confirmed by a pathologist. Each case was calculated for the mean value of the signal intensity of all regions of interest and normalized to the total number of cells/area for statistical analysis. The output of the computerized measurement produced a continuous data ranging from 56 to 70,367 for MAF expression. A cut-off of 1000 OD was chosen on the basis of receiving operating characteristic (ROC) curves.

Reporter assay

Renilla and luciferase reporter assays were performed as previously described [3]. C-MARE sequence was cloned in renilla-expressing vector. For analysis of PTHLH promoter, the

promoter fragments P1 and P2/3 and P1 promoter mutants were cloned into a luciferase reporter construct. A CMV-RFP plasmid (Promega) was included as a control for transfection efficiency.

Osteoclast differentiation assay

In order to isolate bone marrow mononuclear cells, 4- to 6-week-old wild-type C57BL/6 mice were sacrificed and their femora and tibias were flushed with cold PBS solution. Bone marrow mesenchymal cells were then cultured in 100-mm dishes overnight in α-MEM (Invitrogen) media supplemented with 10% fetal bovine serum, 100 U/ml penicillin, 0.1 mg/ml of streptomycin and 0.29 mg/ml of glutamine. Non-adherent cells were collected and plated in the same media. After 2 days the adherent cells were scraped and counted in order to be plated in 24-well dishes. Osteoclast differentiation was induced by adding 20 ng/ml RANKL (peproTech), 30 ng/ml M-CSF (R&D Systems), and conditional media from BC cells. Medium was changed at day 3, and TRAP+ staining (Sigma-Aldridge) was performed at day 6. For PTHrP antagonist treatment, the 7-34 PTHrP peptide (Bachem) (5 μg/ml) was added to the wells.

Cell Migration Assay

Cells were grown until confluence to form a monolayer, after which the ‘scratch‘, wound, was inflicted with a sterile tip. The wound closure was monitored at the given time points and cell migration was calculated as the extent of closure in time.

Adhesion Assay

Bone marrow stromal cells were isolated from the tibia of 6 weeks old mice, as described above, and maintained in alpha-MEM medium. 24 hours prior to the assay, bone marrow cells were seeded in 24-well plate to form a monolayer. Tumor cells were labeled 30 minutes at 37ºC with CellTtracker^{TM} Green CMFDA (Life Technologies). For the adhesion assay tumors cells were trypsinzed and counted so that 50,000 cells were seeded per well. After one hour of

incubation at 37ºC, wells were washed 3 times with PBS and fixed in formalin for 30 minutes at room temperature. The attached cells were quantified under fluorescent microscope. Five fields per well were counted.

Patient Data Sets

Description of the discovery MSKCC/EMC data set

We used the EMC-344 and MSK-82 data sets, which are based on HG-U133A and were combined, and to EMC-189 data set, which is based on HG-U133plus2 and was processed separately (GSE2603, GSE12276, GSE5327, and GSE2034 available at the Gene Expression Omnibus (GEO) public database). In order to remove systematic biases, prior to merging the expression measurements were converted to z-scores for all genes. Patient clinical record of the 615 primary tumor samples has been extracted from Supplementary material described of Zhang, X.H., et al "Latent bone metastasis in breast cancer tied to Src-dependent survival signals" Cancer Cell. 2009, 6: 67-78. Following the indications of the Cancer Cell manuscript (**Supplementary Table 1**), we retrieved the metastasis site annotation from table 8 of Bos, P., et al "Genes that mediate breast cancer metastasis to the brain" Nature. 2009, 459: 1005-9. The metastasis site annotation was reported for 560 of the 615. The median duration of follow-up was 7.667 years (range, 0 to 14.25) for the 268 patients without metastasis and 1.917 years (range, 0 to 9.583) for the 292 patients with metastasis. The median follow-up among all 560 patients was 4 years (range, 0 to 14.25). Those 55 patients with no time to metastasis reported were not included in any ulterior time to metastasis analysis.

To examine the prognostic value of MAF in different subsets of breast cancers, we divided the breast cancer samples based on their ER status. For ER status, we used the intensity of ESR1 on the Affymetrix chip as the pathological status was not available (for GSE12276). The distribution of ESR1 gene showed strong bimodality. We defined the ER+ and ER- tumors based on this bimodality. We defined the ER+ and ER- tumors based on this bimodality (ER+ BC n=349, Figures 1D, 2A, S1F,G and S3E).

Missing Values Report

Five hundred and sixty patients are represented in the cohort. Of which, the variables "ER, "HER2mod", "tumor size" have 15(2%), 20 (3%), and 63 (11%) missing values, respectively.

Description of the validation van de Vijver data set I

As described in van de Vijver et al N Engl J Med 2002; 347:1999-2009, surgical resection specimens from a series of 295 consecutive women with breast cancer were selected from the fresh-frozen–tissue bank of the Netherlands Cancer Institute according to the following criteria: the tumor was primary invasive breast carcinoma that was less than 5 cm in diameter at pathological examination (pT1 or pT2); the apical axillary lymph nodes were tumor-negative, as determined by a biopsy of the infraclavicular lymph nodes; the age at diagnosis was 52 years or younger; the calendar year of diagnosis was between 1984 and 1995; and there was no previous history of cancer, except nonmelanoma skin cancer. All patients had been treated by modified radical mastectomy or breast-conserving surgery, including dissection of the axillary lymph nodes, followed by radiotherapy if indicated. Among the 295 patients, 151 had lymph-node–negative disease (results on pathological examination, pN0) and 144 had lymph-node–positive disease (pN+). Ten of the 151 patients who had lymph-node–negative disease and 120 of the 144 who had lymph-node–positive disease had received adjuvant systemic therapy consisting of chemotherapy (90 patients), hormonal therapy (20), or both (20). Sixty-one of the patients with lymph-node–negative disease were also part of the previous study used to establish the prognosis profile. All patients were assessed at least annually for a period of at least five years. Follow-up information was extracted from the medical registry of the Netherlands Cancer Institute. The median duration of follow-up was 7.8 years (range, 0.05 to 18.3) for the 207 patients without metastasis as the first event and 2.7 years (range, 0.3 to 14.0) for the 88 patients with metastasis as the first event. The median

follow-up among all 295 patients was 6.7 years (range, 0.05 to 18.3). There were no missing data.

Description of the GSE14020

Similarly, GSE14020 data set, which is based on HG-U133A and HG-U133plus2 was analyzed. In order to remove systematic biases, prior to merging the expression measurements were converted to z-scores for all genes. No missing annotations were reported.

Description of the validation Spanish data set II

As described in Rojo F., et al Ann. Oncol. (2012) 23: 1156-1164, surgical resection specimens from primary breast tumors and mammoplasties obtained from Parc de Salut Mar Biobank (MARBiobanc, Barcelona, Spain), Fundación Jiménez Díaz Biobank (Madrid, Spain) and Valencia Clinic Hospital Biobank (Valencia, Spain). Tumor specimens from formalin-fixed paraffin-embedded (FFPE) blocks were retrospectively selected from consecutive breast cancer patients diagnosed between 1998 and 2000, which had the following criteria: infiltrating carcinomas, operable, no neoadjuvant therapy, enough available tissue and clinical follow-up.

TNM (tumor–node–metastasis) staging was classified using the American Joint Committee on Cancer (AJCC) staging system. Histological grade was defined according Scarff–Bloom–Richardson modified by Elston and Ellis, Histopathology (1991) 19: 403-410. ER and PR were determined by immunohistochemistry (IHC) (SP1 and PgR636 clones, respectively; Dako, Carpinteria, CA) establishing positivity criteria in ≥1% of nuclear tumor staining. HER2 amplification was assayed by FISH (Pathvysion; Abbott Laboratories, Abbott Park, IL). Ki-67 was studied by IHC (MIB1 clone; Dako). Patients referred to genetic counseling were studied for BRCA1 and BRCA2 gene status by direct sequencing. The Ethics Committees of the three hospitals approved the study.

Four hundred and fifty six infiltrating carcinomas including 380 IDC (Ductal), 53 ILC (lobular) and 23 of other types were studied. Tissue microarrays (TMA) were constructed as described (Rojo et al Ann. Oncol., 2011). This TMA is an expanded version of that previously described.

In the Spanish validation data set, 38 out of 456 in the TMA (8,3%) patients suffer bone metastasis, which is in the range described in the literature (Jensen et al BMC Cancer 2011). We clarified that in this series, there were a total of 92 relapses (20.1%), and of those, 38 (8.3%) had bone metastasis at any time of relapse (either as the only site, following other sites of relapse or followed by other sites of relapse). Therefore, the proportion of relapsing patients that had bone metastasis was in fact of 38 (41,3%) out of 92 cases, in line with the proportion of bone metastasis expected as first site of relapse in breast cancer.

i. 16q23 Copy variation analysis (FISH)

Missing Values Report

Three hundred and fifty six patients have information on 16q23 FISH in the database. The variables "ER, "PR", "HER2mod", "grade" and "age" have 7(2%), 7(2%), 8(2%), 3(1%), and 13(4%) missing values respectively. 9 (2.5%) lack time to bone metastasis event. As these missing values constitute less than 5% of the sample size, individuals with missing values in these variables are excluded from the analysis. The variable "Ki67 consenso" has 25 (7%) of missing values and these values are also excluded but reported. Effective sample size for the following analyses is 334 patients, of which 47 (14%) have equal or more than 1.5 copies of the 16q23 compared to reference. Effective sample size for the following analyses in ER+ BC is 250 patients.

ii. MAF protein expression (IHC)

Missing Values Report

The exposure of interest, MAF OD, has 63 missing values out of the 456. These cases are not included in the analysis; the remaining sample size is 393 patients. The

variables "ER, "PR", "HER2mod", "grade" and "age" have 5(1%), 5(1%), 10(2.5%), 5(1%), and 17(4%) missing values respectively. 12 (3%) lack time to bone metastasis event. As these missing values constitute less than 5% of the sample size, individuals with missing values in these variables are excluded. After excluding individuals with missing values in the survival covariate, a total sample size of 372 individuals are used in the analysis, of which 70 (19%) have more than 1000OD signal intensity.

Description of the TCGA data set

As described in Cancer Genome Atlas Network Nature 2012; 490, 61-70 surgical resection specimens from 825 primary breast tumors were obtained from several institutions according to the following criteria: the tumor was primary invasive breast carcinoma including T1 to T4. It is not reported in the original publication how patients were surgically and systemically treated. Among the 825 patients, 384 had lymph-node–negative disease (results on pathological examination, pN0) and 405 had lymph-node–positive disease (pN+). Tumor and germline DNA samples were obtained from 825 patients. Different subsets of patients were assayed on each platform: 466 tumors from 463 patients had data available on five platforms including Agilent mRNA expression microarrays (n = 547), Illumina Infinium DNA methylation chips (n = 802), Affymetrix 6.0 single nucleotide polymorphism (SNP) arrays (n = 773), miRNA sequencing (n = 697), and whole-exome sequencing (n = 507). Owing to the short median overall follow up (17 months) and the small number of overall survival events (93 out of 818), survival analyses were not reported in the publication. Last updated version (march 2015, 1079 samples were analyzed; Information at www.cBioportal.org).

Missing Values Report

The variables "ER, "PR", "HER2Final Status" and "age" have 45(5%), 48(6%), 59(7%), and 7 (1%) missing values respectively. There is no time to bone metastasis event, thus bone metastasis was not analyzed. 1079 (last update March 2015) patients

have CNA information on 16q23.2 region (including MAF gene) in the database, of which 98 (9.1%) are annotated to have a gain or an amplification of the 16q23.2 region compared to reference.

Statistical Methods

A) Cumulative incidence.

For Figures 1F, 2A, and 2C and Supplementary Figures S1F, S1I, S1K and S2H, p-values were obtained after fitting Cox proportional hazard models and performing likelihood ratio tests. Of note, cumulative incidence when using validation data set II was calculated using Cox cause-specific hazard model with competing events (death).

Cumulative incidence functions for recurrence were estimated. These functions estimate the actual percentage of patients who will experience the various competing events within the study cohorts as opposed to the overestimated percentages obtained with the Kaplan-Meier method based on the cause-specific hazards.

Differences between the cumulative incidence functions according to patient subgroups were tested for statistical significance. Analyses were conducted to determine whether the risk of recurrence in bone at any time increased according to baseline characteristics. A cumulative incidence function regression model, Cox regression of cause-specific hazards, was used for multiple regression analyses. Covariates included in the model were nodal status, tumor size and tumor grade. To assess statistical significance of each factor in the multivariate Cox regression model we used likelihood ratio tests, including all other factors in the model.

Kaplan-Meier.

For Figures 1A, 3C, 3D, 3E, 6A, 6B and S1H, p-values were obtained using log-rank tests.

B) Statistical group comparison.

Statistics were calculated by means of a Wilcoxon two-sided test unless indicated.

C) Survival analysis (mRNA, Figure S2E).

A multivariate Cox proportional hazard model was fitted to test the correlation between high MAF-expressing versus the rest of the tumors and bone metastasis. Tumor size, lymph node

status, tumor grade, and proliferation were used as adjustment variables. R's function step was used to perform backward elimination by AIC. P-values were obtained with Cox proportional hazards likelihood ratio tests.

D) Comparison of baseline characteristics (Supplementary Tables 1 and 4).

Differences in age were checked with the Student's t test. All other variables were tested with Fisher's exact test.

E) Measure of agreement (Figure 2D)

We assessed the agreement of IHC and FISH events in each sample. A Wilcoxon rank-sum test was used.

Measure of correlation (Figure S2G)

We assessed the correlation of IHC and FISH events in each sample. A Pearson r correlation coefficient was used.

F) Diagnostic performance of FISH and IHC (Tables 1, 2 and Supplementary Tables 1, 2, 4, 5, Supplementary Figure 2C).

- A multivariate Cox cause-specific hazard model with competing events (death) was fitted to test the correlation between 16q23 or MAF and bone metastasis. Tumor size, lymph node status, tumor grade, Her2, and proliferation were used as adjustment variables. Diagnostic performance was evaluated by comparing the AUC of the ROC curves.

- Sensitivity (Se), specificity (Sp), positive predictive value (PPV), and negative predictive value (NPV) were computed for each of the classification categories on the basis of the most predictive variables (16q23 FISH and MAF IHC). Bootstrapping of the PPV and NPV was done.

G) Prognostic role.

- Cox regression modeling of the outcome "time to bone metastasis" was done with by "efron" management of ties. A maximum of 1 variable for every 5-10 events was considered.

Categories of Sites of recurrence

Different estimates were used depending on the data set.

For the MSKCC/EMC, all recurring breast cancer events reported were classified according to their sites, as follows: bone metastasis, lung metastasis, brain metastasis if this event is reported irrespectively of other metastasis sites reported at the same time. Time to event was defined as time from surgical resection to occurrence of event.

For the Spanish Data set, all recurring breast cancer events reported were classified according to their sites, as follows: local recurrences, confined to the ipsilateral chest wall and including mastectomy scars; regional recurrences, including ipsilateral axillary, internal mammary lymph node metastasis; distant recurrences in soft tissue; bone metastases; and visceral metastasis, including all other organ involvement metastasis. Other events were also recorded and this event is reported. Time to event was defined as time from surgical resection to occurrence of event.

Because special emphasis was being placed on the incidence of recurrence in bone, occurrence of bone metastases with or without recurrence at any other site or subsequent bone metastasis after recurrence at any other site was classified as the event of interest. Time to recurrence in bone at any time was defined as the time from tumor ressection to the first or subsequent event in bone after a metastasis elsewhere, whichever occurred first. Death before recurrence in bone was considered the only competing event in this analysis.

In a subset analysis, interest is placed on the incidence of visceral and soft tissue metastasis. Occurrence of bone metastases without recurrence at any other site or death before recurrence in soft tissue was considered the only competing event in this analysis. Otherwise, patients' data were censored at the time they were last known to be alive without recurrence in soft tissue metastasis.

Analyses of the association between 16q22-24 and bone metastasis in MSKCC/EMC data set

For every ER+ sample in the cohort (n=349) we select the genes in the cohort that belong to

16q22-16q24 (169 genes). We test if the average expression of these genes is different form 0 using a one-sided Wilcoxon test where the alternative hypothesis is that the average expression is bigger than 0.

The samples with a p-value for the test below 0.05 are considered CNA. The rest are considered no CNA. We fit a Cox proportional hazards model to see how well this grouping predicts overall metastasis. We obtained a hazard ratio for CNA vs. no CNA of 1.37 (1.01-1.88) with a p-value of 0.04849

Evaluation of the biomarker in the adjuvant setting

The efficacy of treatments in the adjuvant setting is usually analyzed in a "relapse event-free survival" manner in randomized clinical trials. This analysis considers both relapse (bone metastasis in our case) and death as events of same relevance (FDA guidelines). To mimic this analysis, we provide below an analysis of bone metastasis-free survival for both CNA and MAF IHC.

Multivariate analysis of bone metastasis-free survival (models are adjusted by tumor size, affected lymph nodes, grade and ki67 proliferation rate) based on the Spanish data set.

	HR (95% CI)	P value
16q23 CNA negative	1 (Ref.)	
16q23 CNA positive	4.17 (2.12-8.20)	3.5e-5
IHC MAF LOW	1 (Ref.)	
IHC MAF HIGH	2.81 (1.72-4.59)	3.7e-5

Evaluation of the 16q23 chromosomal gain frequency based on the TCGA consortium breast cancer data set

16q23 Chromosomal gains frequency estimation was based on genes within each segment using the "The Cancer Genome Atlas (TCGA) breast cancer project" data. DNA copy-number changes of each gene were evaluated using Level 3 GISTIC data (high level amplification, low level amplification, neutral, low level deletion and high level deletion) that is publicly available at the TCGA portal (https://tcga-data.nci.nih.gov/tcga/).

As described in "Comprehensive molecular portraits of human breast tumours" Nature 2012, DNA from each tumor or germline-derived sample was hybridized to the Affymetrix SNP 6.0 arrays using protocols at the Genome Analysis Platform of the Broad Institute. From raw .CEL files, Birdseed was used to infer a preliminary copy-number at each probe locus28. For each tumor, genome-wide copy number estimates were refined using tangent normalization, in which tumor signal intensities are divided by signal intensities from the linear combination of all normal samples that are most similar to the tumor. This linear combination of normal samples tends to match the noise profile of the tumor better than any set of individual normal samples, thereby reducing the contribution of noise to the final copy-number profile. Individual copy-number estimates then undergo segmentation using Circular Binary Segmentation. As part of this process of copy-number assessment and segmentation, regions corresponding to germline copy-number alterations were removed by applying filters generated from either the TCGA germline samples from the ovarian cancer analysis or from samples from this collection.

Segmented copy number profiles for tumor and matched control DNAs were analyzed using Ziggurat Deconstruction, an algorithm that parsimoniously assigns a length and amplitude to the set of inferred copy number changes underlying each segmented copy number profile. Analysis of broad copy number alterations was then conducted as previously described. Significant focal copy number alterations were identified from segmented data using GISTIC 2.0. NMF consensus clustering of copy number data was performed using the presence or absence of amplifications or deletions in regions identified by GISTIC 2.0 analysis.

Chromosomal region gain	Frequency (n=1079)	Percentage
16q23.2 (MAF gene included)	98	9.1

References

1. Minn AJ, Gupta GP, Siegel PM, *et al.* Genes that mediate breast cancer metastasis to lung. Nature 2005;436(7050):518-24.
2. Kang Y, Siegel PM, Shu W, *et al.* A multigenic program mediating breast cancer metastasis to bone. Cancer Cell 2003;3(6):537-49.
3. Tarragona M, Pavlovic M, Arnal-Estape A, *et al.* Identification of NOG as a specific breast cancer bone metastasis-supporting gene. J Biol Chem 2012;287(25):21346-55.
4. Gentleman RC, Carey VJ, Bates DM, *et al.* Bioconductor: open software development for computational biology and bioinformatics. Genome Biol 2004;5(10):R80.
5. Irizarry R, Hobbs, B., Collin, B., Beazer-Barclay, Y.D., Antonellis, K.J., Scherf, U. and Speed, T.S. . Exploration, normalization, and summaries of high density oligonucleotide array probe level data. Biostatistics 2009;4:249-264.
6. Rossell D, Guerra, R. and Scott, C. . Semi-parametric differential expression analysis via partial mixture estimation. Statistical Applications in Genetics and Molecular Biology 2008;7:1-15.
7. Smyth GK. Limma: linear models for microarray data. In: Gentleman R, Carey, V., Dudoit, S., Irizarry, R. and Huber, W. , (ed). *Bioinformatics and Computational Biology Solutions using R and Bioconductor*. New York: Springer; 2005, 397-420.
8. Hu G, Chong RA, Yang Q, *et al.* MTDH activation by 8q22 genomic gain promotes chemoresistance and metastasis of poor-prognosis breast cancer. Cancer Cell 2009;15(1):9-20.
9. Venkatraman ES, Olshen AB. A faster circular binary segmentation algorithm for the analysis of array CGH data. Bioinformatics 2007;23(6):657-63.
10. Arnal-Estape A, Tarragona M, Morales M, *et al.* HER2 silences tumor suppression in breast cancer cells by switching expression of C/EBPss isoforms. Cancer Res 2010;70(23):9927-36.

Supplementary Table 1. Baseline Characteristics According to 16q23 CNA. Differences in age were checked with the Student's t test. All other variables were tested with Fisher's exact test.

	Complete series (n=334)		16q23 CNA < 1.5 (n=279)		16q23 CNA > or =1.5 (n=55)		
Characteristics	No. of patients	%	No. of patients	%	No. of patients	%	*P*
Age (median, range)	58, 26-90		58, 31-90		58, 26-90		
Menopausal status							0.632
Premenopausal	104	31.1	85	30.5	19	34.5	
Postmenopausal	230	68.9	194	69.5	36	65.5	
Tumor size, mm							0.008
≤20	204	61.0	179	64.2	25	45.4	
21-50	100	30.0	80	28.7	20	36.4	
>50	30	9.0	20	7.1	10	18.2	
Tumor grade							0.011
I	57	17.0	52	18.6	5	9.1	
II	159	47.6	138	49.4	21	38.2	
III	118	35.3	89	32.0	29	52.7	
Lymph nodes							0.091
None	203	60.7	175	62.7	28	50.9	
1-3	86	25.7	72	25.8	14	25.4	
4-9	29	8.6	21	7.5	8	14.6	
>9	16	4.7	11	4.0	5	9.1	
Estrogen receptor status							0.174
Negative	84	25.1	66	23.7	18	32.7	
Positive	250	74.9	213	76.3	37	67.3	
Progesterone receptor status							0.282
Negative	118	35.3	95	34.0	23	41.8	
Positive	216	64.6	184	66.0	32	58.2	
HER2 status							0.850
Negative	271	81.2	227	81.4	44	80.0	
Positive	63	18.8	52	18.6	11	20.0	
Bone mets at any time							9e-12
Negative	306	91.6	271	97.13	35	63.64	
Positive	28	8.4	8	2.87	20	36.36	
(median follow up, months)			7.1		6.9		
Soft and visceral metastasis before bone mets or death							0.998
Negative	318	95.2	265	94.9	53	96.3	
Positive	16	4.7	14	5.0	2	3.6	
Proliferation (Ki-67)							0.005
Low proliferation (<15%)	229	68.5	200	71.7	29	52.7	
High proliferation (≥15%)	84	25.1	62	22.22	22	40.0	
Proliferation (n.a.)	21	6.2	17	6.1	4	7.3	

Abbreviations: HER2, human epidermal growth receptor 2, n.a. not available

Supplementary Table 2.
Competing risk (death before recurrence in bone) survival analysis complementing Table 1

	Univariate (n=306)			Multivariate (n=306)		
Variable	HR	95% CI	*P*	HR	95% CI	*P*
Menopausal status			0.550			-
Premenopausal	1.00			-		
Postmenopausal	1.32	0.51 to 3.43		-	-	
Tumor size, mm			0.038			0.150
≤20	1.00			1.00		
21-50	1.63	0.68 to 3.91		2.23	0.71 to 6.94	
>50	3.20	1.16 to 8.81		4.08	0.99 to 16.80	
Tumor grade			0.039			0.069
I	1.00			1.00		
II	0.40	0.15 to 1.05		1.47	0.17 to 12.54	
III	2.97	1.22 to 7.21		4.39	0.52 to 36.43	
Lymph nodes			0.107			0.626
None	1.00			1.00		
1-3	0.74	0.27 to 2.02		0.74	0.22 to 2.48	
4-9	1.68	0.47 to 5.97		0.70	0.14 to 3.42	
>9	4.73	1.57 to 14.18		1.76	0.41 to 7.43	
Hormonal receptor status			0.081			-
Negative	1.00			-		
Positive	0.45	0.18 to 1.08		-	-	
HER2 status			0.105			-
Negative	1.00			-		
Positive	2.20	0.88 to 5.47		-	-	
Proliferation (Ki-67)			0.347			0.163
Low proliferation (<15%)	1.00			1.00		
High proliferation (≥15%)	0.57	0.16 to 1.97		0.41	0.13 to 1.55	
16q23 (FISH CNA)			0.936			0.748
Below 1.5	1.00			1.00		
Equal or More 1.5	0.95	0.27 to 3.28		0.59	0.16 to 2.18	

Abbreviations: HR, hazard ratio; CI, confidence interval; HER2, human epidermal growth factor receptor 2

Supplementary Table 3.
Baseline Characteristics According to MAF IHC expression

Characteristics	Complete series (n=372)		MAF non-overexpression (n=301)		MAF overexpression (n=71)		*P*
	No. of patients	%	No. of patients	%	No. of patients	%	
Age (median, range)	58, 26-90		58, 31-90		59, 26-90		
Menopausal status							0.772
Premenopausal	109	29.3	87	28.9	22	31.0	
Postmenopausal	263	70.7	214	71.1	49	69.0	
Tumor size, mm							0.429
≤20	206	55.3	165	54.8	41	57.7	
21-50	130	35.0	109	36.2	21	29.6	
>50	36	9.7	27	9.0	9	12.7	
Tumor grade							0.799
I	67	18.0	56	18.6	11	15.5	
II	178	47.8	144	47.8	34	47.9	
III	127	34.2	101	35.5	26	36.6	
Lymph nodes							0.369
None	222	59.7	177	58.8	45	63.4	
1-3	90	24.2	78	25.9	12	16.9	
4-9	37	9.9	28	9.3	9	12.7	
>9	23	6.2	18	6.0	5	7.0	
Estrogen receptor status							0.764
Negative	95	25.5	76	25.2	19	26.8	
Positive	277	74.5	225	74.8	52	73.2	
Progesterone receptor status							0.679
Negative	132	35.5	105	34.8	27	38.0	
Positive	240	64.5	196	65.2	44	62.0	
HER2 status							0.326
Negative	296	79.6	236	78.4	60	84.5	
Positive	76	20.4	65	21.6	11	15.5	
Bone mets at any time							6e-5
Negative	342	91.9	286	95.0	56	78.9	
Positive	30	8.1	15	5.0	15	21.1	
(median follow up, months)			7.6		6.9		
Soft and visceral metastasis before bone or death							0.355
Negative	354	95.1	288	95.7	66	92.9	
Positive	18	4.8	13	4.3	5	7.1	
Proliferation (Ki-67)							0.100
Low proliferation (<15%)	272	73.1	226	75.1	46	64.8	
High proliferation (≥15%)	100	26.9	75	24.9	25	35.2	

Abbreviations: HER2, human epidermal growth factor receptor 2

Supplementary Table 4.
Competing risk (death before recurrence in bone) survival analysis in patients complementing Table 2. Differences in age were checked with the Student's t test. All other variables were tested with Fisher's exact test.

	Univariate (n=342)			Multivariate (n=342)		
Variable	HR	95% CI	*P*	HR	95% CI	*P*
Menopausal status			0.12			-
Premenopausal	1.00			-		
Postmenopausal	1.94	0.78 to 4.79		-	-	
Tumor size, mm			0.002			0.054
≤20	1.00			1.00		
21-50	1.96	0.94 to 4.09		2.62	1.06 to 6.50	
>50	2.59	1.05 to 6.39		3.55	1.08 to 11.69	
Tumor grade			0.024			0.263
I	1.00			1.00		
II	0.67	0.31 to 1.43		1.08	0.29 to 4.01	
III	2.03	0.97 to 4.22		2.05	0.55 to 7.61	
Lymph nodes			0.203			0.671
None	1.00			1.00		
1-3	1.11	0.49 to 2.51		1.32	0.53 to 3.25	
4-9	1.40	0.48 to 4.05		0.84	0.24 to 2.88	
>9	2.70	0.94 to 7.78		1.85	0.55 to 6.15	
Hormonal receptor status			0.029			-
Negative	1.00			-		
Positive	0.43	0.20 to 0.89		-	-	
HER2 status			0.163			-
Negative	1.00			-		
Positive	1.79	0.81 to 3.94		-	-	
Proliferation (Ki-67)			0.282			0.080
Low proliferation (<15%)	1.00			1.00		
High proliferation (≥15%)	0.60	0.23 to 1.58		0.43	0.15 to 1.18	
cMAF (IHC)			0.624			0.637
Non-overexpression	1.00			1.00		
Overexpression	1.25	0.51 to 3.09		1.24	0.50 to 3.06	

Abbreviations: HR, hazard ratio; CI, confidence interval; HER2, human epidermal growth factor receptor 2

Supplementary Figure 1

A) Tumor growth from Parental and BoM2 cells injected orthotopically in mouse mammary fat pad was scored. Data is presented as tumor volume for individual tumors from each experimental group. P-value scored by two-sided Wilcoxon signed-rank test.

B) *CCND1 and cMYC* expression levels measured by qRT-PCR in the presence of estradiol or tamoxifen for 24h, as indicated, and normalized to *B2M* levels. Data is presented as mean of three independent experiments with S.D.

C) Tumor growth of subcutaneous tumors from BoM2 cells with or without estrogen supply was scored by measuring tumor volume. Data is mean with sd. (n=3). P-value scored by two-sided Wilcoxon signed-rank test.

D) CGH analysis of BoM2 and Parental cells. Genetic gains and losses in BoM2 comparing to Parental cells, for each chromosome, are depicted with red and green color bars respectively.

E) Analysis of copy number association with metastasis based on gene expression (ACE-like Algorithm, R phenoTest package). Colored area depicts genomic areas were increase or decrease gene expression is significantly ($p<0.05$) associated with metastasis in ER+ breast cancer tumors (discovery MSKCC/EMC data set). These plots focus on potential deletion on chromosome 6, 12, 19, 20 and 21.

F) Cumulative incidence plot of metastasis using ER+ BC primary tumors from the MSKCC/EMC data set. Patients were divided between 16q22-24 CNA negative or positive groups based on significant gain in this region compared to mean of all tumors. HR-hazard ratio. CI-95% Confidence Interval. P-values were obtained using Cox proportional hazard model.

G) Kernel density plots representing the density of the various 16q23 genomic region copy number populations in breast cancer cells lines. Cut off of 1.5 for 16q23/16q11.2 ratio was used to score copy number gain and it is depicted with red dashed line. The percentage of cells carrying 16q23 copy number gain is shown for each cell line. Representative images of FISH stained ZR-75 and

T47D cells using a 0.2Mb 16q23 FISH probe centered on *MAF* gene locus and CEP16 (16q11.2) probe for normalization are shown. Scale bar 10 μM.

H) Kaplan-Meier curve of overall survival in the Validation data set II (Spanish BC human primary tumor data set, n=334). P-value was obtained using log-rank test. Patients were stratified according to 16q23/CEP16 as CNA negative (<1.5) and 16q23/CEP16 CNA positive (> or = 1.5) group based on cut-off of 1.5 16q23/CEP16 copies per cell. A minimum of 50 cells per core and 3 cores per tumor were scored.

I) Cumulative incidence of soft and visceral tissue metastasis using death or bone metastasis before recurrence in soft and visceral metastasis as a competing event was used in Spanish data set. Patients were divided between 16q23 CNA negative and 16q23 CNA positive group based on cut-off of 1.5 16q23/CEP16 copies per cell. A minimum of 50 cells per core and 3 cores per tumor were scored. HR-hazard ratio. CI- 95% Confidence Interval. P-values were obtained after fitting Cox proportional hazard model with competing events.

J) (Up), Receiver Operating Characteristic (ROC) curves for diagnostic performance of 16q23 amplification for bone metastasis ever and as a first site. In a ROC curve the true positive rate (Sensitivity) is plotted in function of the false positive rate (100-Specificity) for different cut-off points. Each point on the ROC curve represents a sensitivity/specificity pair corresponding to a particular decision threshold. (Down), Table that represents bone metastasis diagnostic performance of 16q23 amplification (bone metastasis ever) measured by FISH. Se-Sensitivity, Sp-Specificity, PPV-positive predictive value and NPV-negative predictive value.

K) Cumulative incidence plots of bone metastasis at any time using death before recurrence in bone as a competing event for TN and HER2+ BC patients in Spanish data set. Patients were divided between 16q23 CNA negative and 16q23 CNA positive group based on cut-off of 1.5 16q23/CEP16 copies per cell. A minimum of 50 cells per core and 3 cores per tumor were scored. Please note that the numbers are small and make the estimates imprecise. HR-hazard ratio. CI-95% Confidence Interval. P-values were obtained after fitting Cox proportional hazard model with competing events.

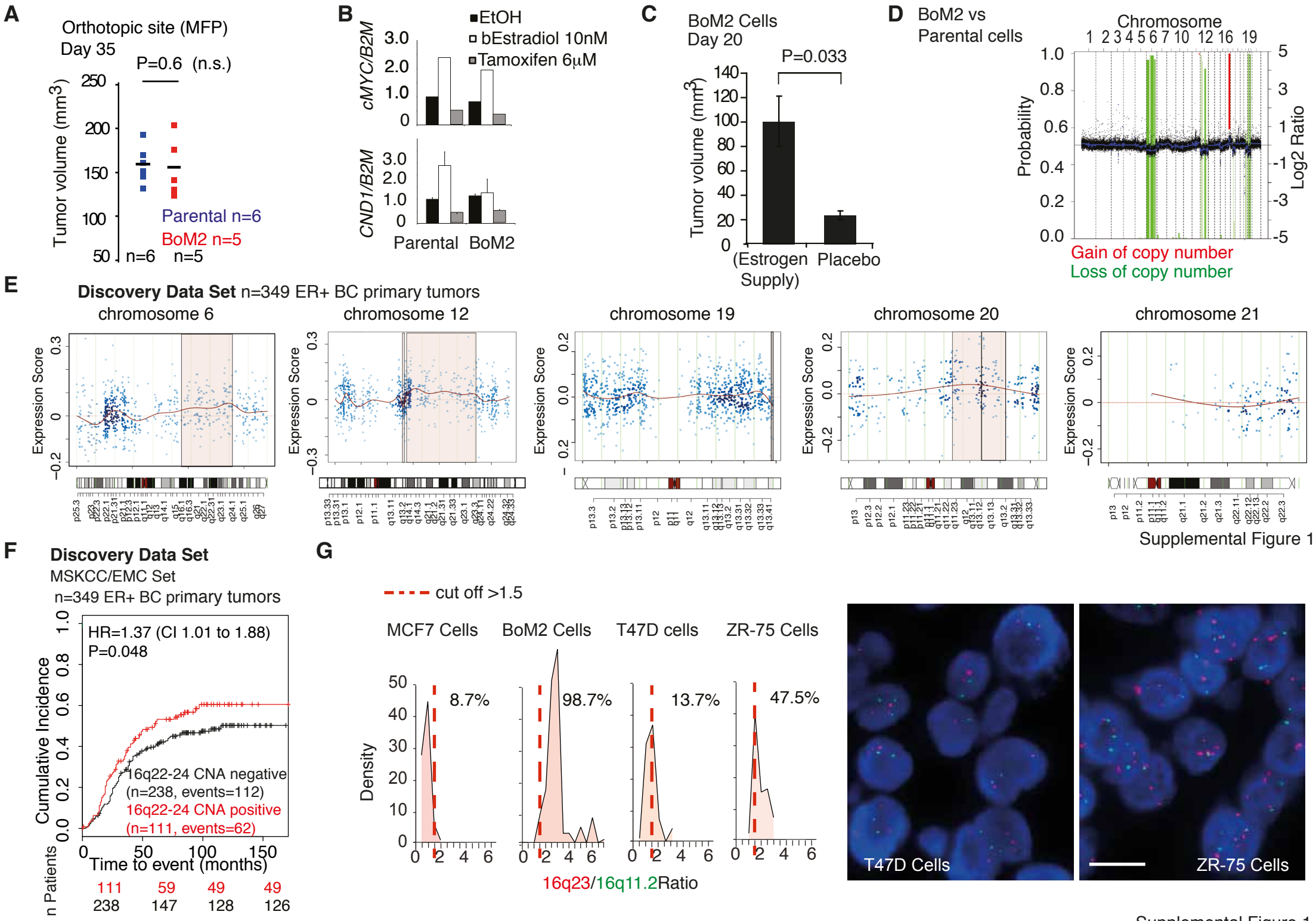

Supplemental Figure 1

Supplemental Figure 1

H

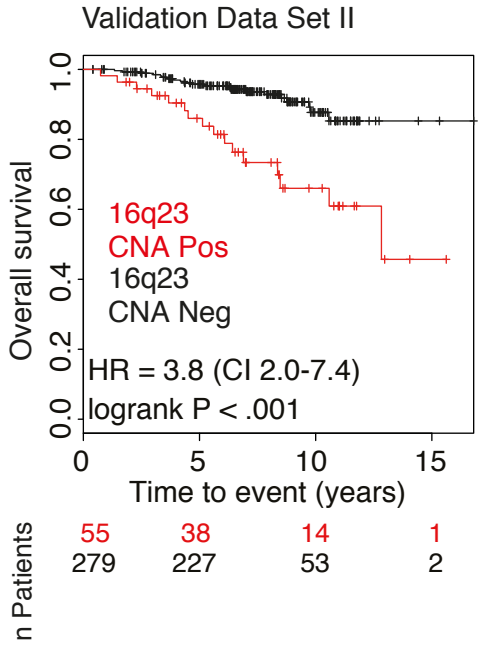

J

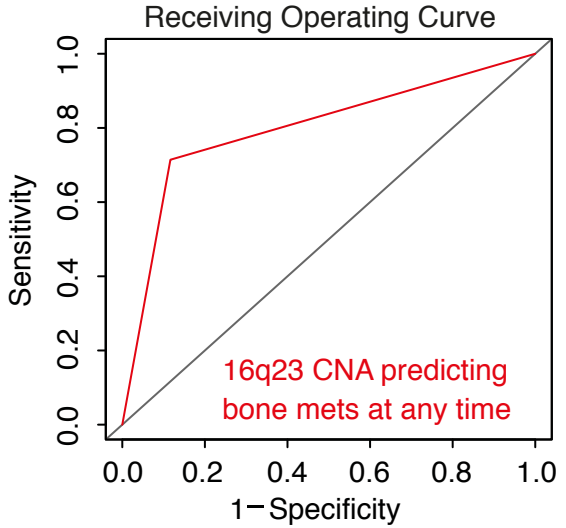

Diagnostic performance of 16q23 / CEP16 CNA
(bone mets at any time)

Sample				Bootstrap	
Se	Sp	PPV	NPV	PPV (5%-95%)	NPV (5%-95%)
71	88	36	97	36 (25-46)	97 (95-99)

I

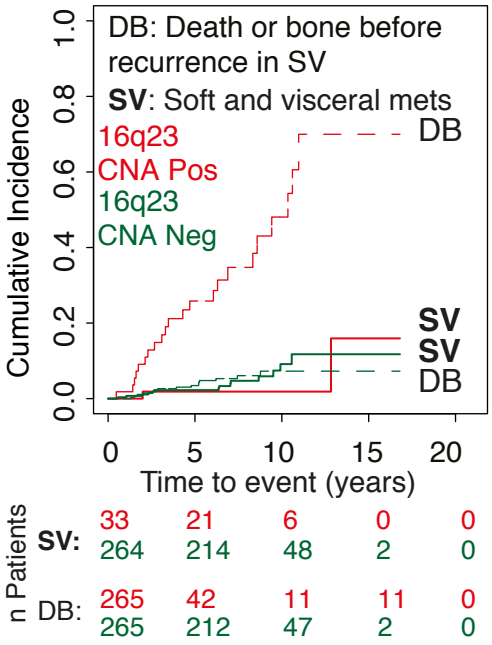

K

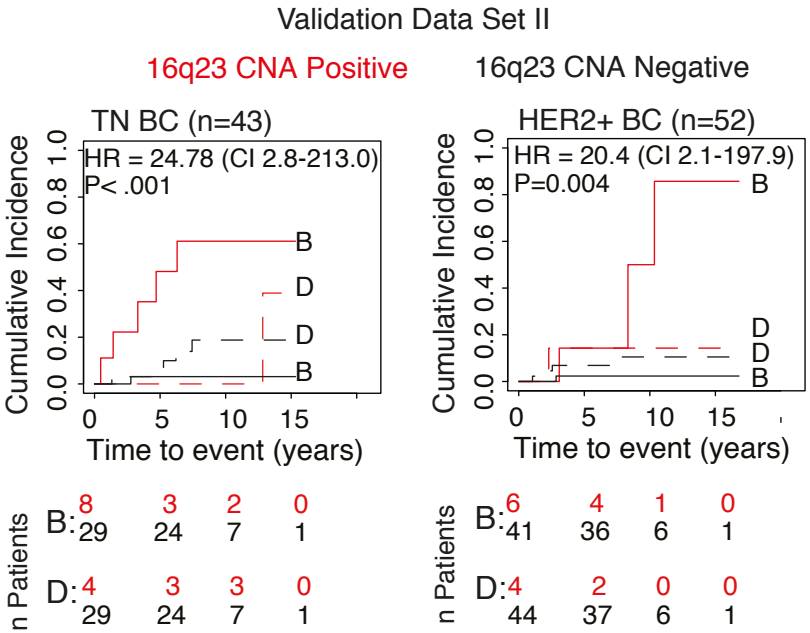

D: Death before recurrence in bone
B: Bone mets at any time

Supplemental Figure 1

Supplementary Figure 2

A) Plot depicts a schematic representation of the chromosome 16. In red highlighted the region and genes encoded within the 16q22-24. Among them, in green those genes that are significantly differentially expressed (absolute fold change bigger than 2 and Bayesian FDR below 5%) in BoM2 compared to parental MCF7 cells (C).

B) Principal component analysis (PCA) based on gene expression profiles segregated parental MCF7 cells from BoM1 and BoM2 populations based on the genetic variability. The Principal component 1 (PC1) captured the bone metastasis tropism phenotype.

C) Comparative genome-wide expression analysis demonstrated that 511 genes were differentially expressed at least 2-fold in highly bone metastatic derivatives.

D) Gene list highlighting the 6 genes differentially expressed with a Bayesian FDR below 5% in BoM derivatives compared to parental cells located at the Chromosome 16. In green, genes located in 16q22-24.

E) Univariate and multivariate analysis of different covariates association, including MAF gene expression, with bone metastasis using the discovery MSKCC/EMC data set. P-values were obtained with Cox proportional hazards likelihood ratio tests.

F) Plot depicts MAF protein expression (OD) in a cohort of 372 primary breast cancer tumors (validation Spanish data set). Tumors are segregated according to BC subtype (ER+, HER2+ and TN). Red tick depicts tumors from patients that eventually developed bone metastasis. OD-optical density based on MAF immunostaining. 15 MAF positive tumors developed bone metastasis (PPV=21), while 14 did in the MAF negative group (PPV=4.5)

G) Plot with the MAF protein score (IHC, Optical Density values) on the vertical axis and log MAF copy number ratio (16q23/CEP16) on the horizontal axis per each BC sample analyzed in the Spanish validation set. Pearson r correlation coefficient is determined.

H) Cumulative incidence plot of bone metastasis at any time, considering death before recurrence in bone as a competing event, in ER+ (Left) and TN (Right) BC patients in Spanish data set. MAF

cut-off is indicated in each plot. P-values were obtained after fitting Cox proportional hazard model with competing events.

I) Table shows Hazard Ratio for bone metastasis at any time, using death before recurrence in bone as a competing event, and its p-value of high MAF protein expression (OD>1000) group compared to MAF low group in different BC subtypes in Spanish data set.

A

Genes and MIR encoded at 16q22-24 region

Chromosome 16 Position

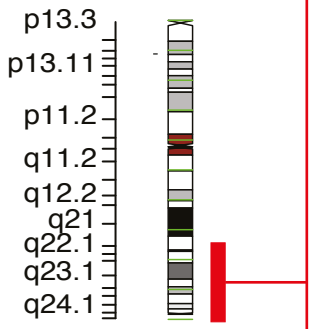

Genes significantly differentially expressed more than 2 fold in BoM2 compared to Parental

CLEC18B	EDC4	CLEC18C	DUS2L
HSF4	ADAT1	MLKL	CMTM4
LRRC36	ANKRD11	ZCCHC14	DHODH
SPG7	AGRP	HSD11B2	PDF
FAM65A	CDH13	CES3	DNAAF1
FTSJD1	CLEC3A	NIP7	ZDHHC1
CBFB	PDP2	TRAPPC2L	ATP6V0D1
AFG3L1P	CIRH1A	CTRL	TXNL4B
NAE1	FLJ30679	CTRB1	LOC732275
PLEKHG4	CFDP1	SPIRE2	BCMO1
TMCO7	MON1B	DYNLRB2	SYCE1L
PARD6A	WWP2	USP10	TAT
APRT	HP	LOC1002870	MPHOSPH6
FBXO31	DDX19A	36	WDR59
SLC12A4	PSMD7	NUTF2	GSE1
CALB2	CMIP	VPS4A	NECAB2
CDK10	SLC7A6	LOC400548	KIAA1609
MVD	RRAD	LOC1001308	CTU2
TUBB3	B3GNT9	94	SLC38A8
CES4A	ATXN1L	GCSH	CHTF8
ESRP2	LRRC29	TSNAXIP1	KIAA0895L
CBFA2T3	SNAI3-AS1	PIEZO1	KIAA0513
JPH3	TERF2	ACSF3	C16orf55
HYDIN	RPL13	HPR	SLC7A6OS
MTHFSD	SF3B3	TMEM170A	ZFP1
ZNF778	IST1	PSMB10	PKD1L3
DDX19B	CES2	HSD17B2	MAF
CENPBD1	CCDC79	PLCG2	SNORD111B
HSBP1	AARS	TRADD	PLA2G15
IL34	WFDC1	TMEM231	C16orf86
ZDHHC7	ENKD1	LINC00304	RLTPR
ST3GAL2	FUK	CDH15	MIR328
DYNC1LI2	VAC14	ATP2C2	OSGIN1
WWOX	SNTB2	MIR1910	PABPN1L
NFAT5	MARVELD3	ZFHX3	GINS2
CENPT	CA5A	FHOD1	COX4I1
TAF1C	CYBA	NUDT7	CYB5B
DEF8	CHST5	COG8	LOC1005061
FAM96B	MIR1538	FOXF1	72
LCAT	BANP	FOXL1	ZNRF1
CHMP1A	HTA	CDH3	MIR1972-1
KARS	CLEC18A	MC1R	CMC2
MAP1LC3B	PRDM7	FOXC2	LINC00311
DPEP3	BCAR1	EMC8	MIR1972-2
DPEP2	FANCA	RNF166	LOC1001296
GLG1	EXOC3L1	DPEP1	17
C16orf70	LOC1005060	SLC7A5	LOC1005060
PSKH1	60	COG4	83
E2F4	SNORD111	ZFPM1	LOC146513
MBTPS1	SNORD71	PKD1L2	MIR140
HAS3	LOC283922	ZNF469	MIR4722
IL17C	FBXL8	HSDL1	MIR4720
DDX28	SNORD68	ELMO3	MIR4719
ADAD2	GALNS	KCTD19	SDR42E1
ZNF821	DHX38	PDXDC2P	SNAI3
AP1G1	SLC22A31	SMPD3	MIR5093
CA7	FOXF1-AS1	IRF8	MIR5189
ADAMTS18	CDH16	COTL1	ZC3H18
EXOSC6	MLYCD	LOC1001288	TMED6
CNTNAP4	C16orf3	81	KCNG4
C16orf46	NOL3	CDT1	MTSS1L
NFATC3	PHLPP2	TCF25	LOC400558
SLC9A5	RANBP10	THAP11	SNORA70D
CDYL2	GAS8	ZFP90	NRN1L
SPATA2L	LOC1001300	PDPR	
TMEM208	15	NQO1	
CDH1	CTRB2	MIR3182	
CPNE7	CHST4	NOB1	
FAM92B	ZNF276	KLHDC4	
FA2H	CHST6	PRMT7	
VAT1L	ACD	RFWD3	
ZNF19	TPPP3	ATMIN	
TERF2IP	DBNDD1	C16orf95	
GAN	GABARAPL2	PMFBP1	
GFOD2	C16orf74	KLHL36	
CENPN	LDHD	CTCF	
VPS9D1	CRISPLD2	ZNF23	

B

Principal Component Analysis

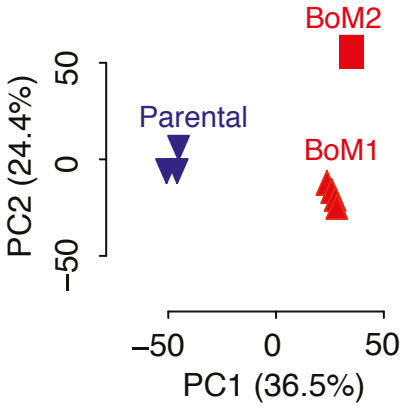

C

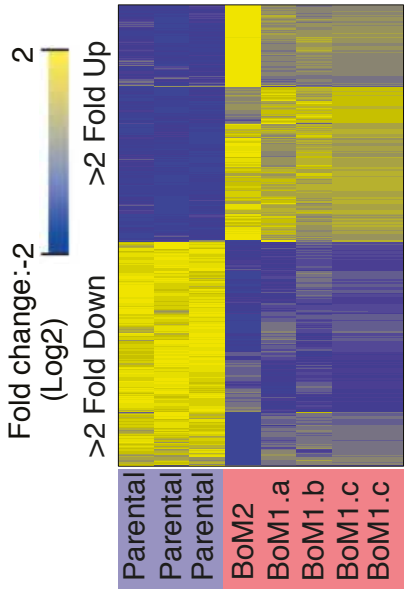

D

Genes differentially expressed in BoM2 vs Parental and located at Chr16

"Chromosome"	"Postion" Start	End	Entrez id	Symbol
16	17196183	17564738	64131	XYLT1
16	18995432,5	19075260	79905	TMC7
16	30542780	30546194	65988	ZNF747
16	56691855	56693214	4494	MT1F
16	67282855	67306093	6553	SLC9A5
16	79627746	79634622	4094	MAF

E

Expression ER+ samples

Univariate analysis with all variables:

	HR	CI.low	CI.up	Pvalue
MAF.HighvsRest	2.55	1.71	3.82	2e-5
pr.1vs0	1.19	0.79	1.80	0.39
her2.1vs0	1.14	0.70	1.85	0.59
age (+1SD)	1.07	0.89	1.28	0.46
size (+1SD)	1.09	0.92	1.31	0.33

pr= Progesteron receptor
her2= HER2 receptor
1=positive
0=negative
MAF.High= MAF levels above mean+sd

Multivariate analysis

	HR	CI.low	CI.up	Pvalue
MAF.HighvsRest	2.59	1.59	4.21	3e-4
pr.1vs0	1.31	0.81	2.11	0.26
her2.1vs0	1.36	0.77	2.39	0.30
age (+1SD)	1.01	0.82	1.25	0.91
size (+1SD)	1.14	0.91	1.43	0.26

Supplemental Figure 2

F

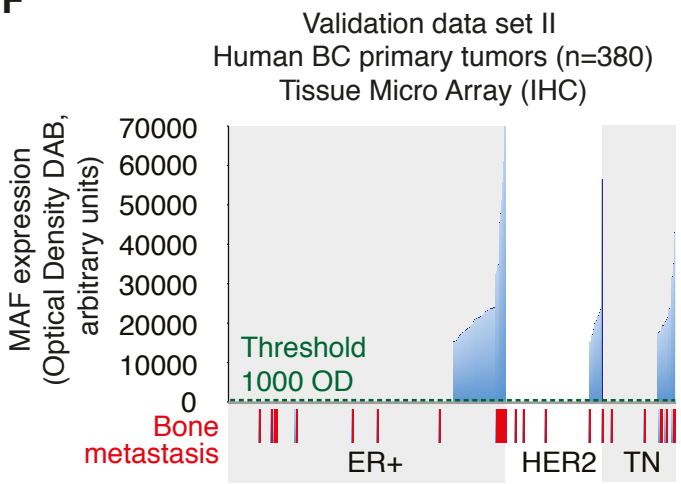

G

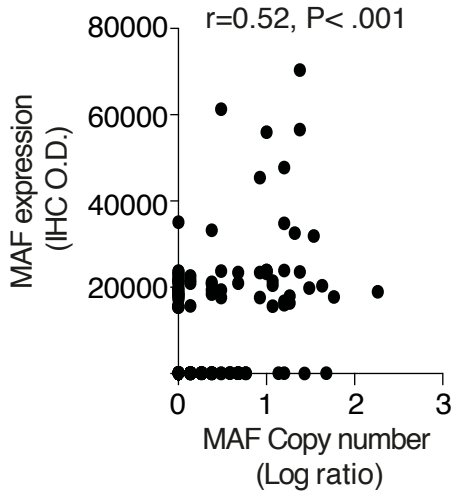

H

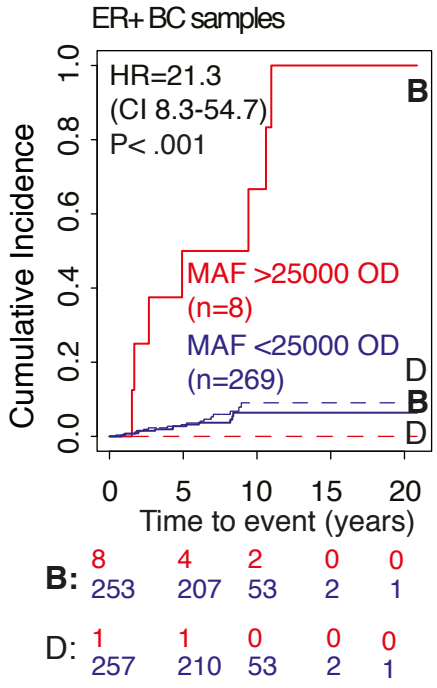

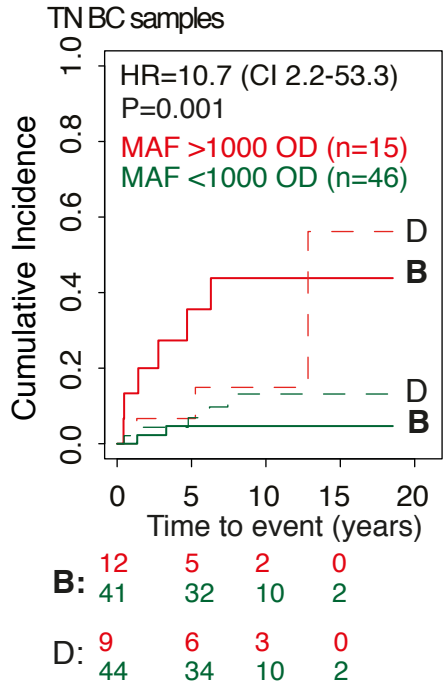

B: Bone mets at any time

D: Death before recurrence in the bone

I

Hazard Ratio (Bone mets at any time)
(Using Death as a competing event)
(MAF positive > 1000 OD)

	HR	CI.low	CI.up	Pvalue
ER+ patients (n=235)	2.7	1.1	6.9	0.04
TN patients (n=62)	10.7	2.2	53.3	0.001
Her2+ patients (n=77)	2.1	0.2	19.3	0.53

Supplementary Figure 3

A) MAF protein in human primary tumor samples and BC cell lines detected by western blot analysis. 16q23 gain positive BC samples and cell lines are shown on top (Red box) whereas 16q23 gain negative BC samples (Grey box) and cell lines at the bottom.

B) Western Blot depicting MAF protein levels in Parental, BoM2, T47D and ZR-75-1 breast cancer cell lines. MAF protein isoforms are distributed between 37 kDa and 50 kDa. α-TUBULIN was used as loading control.

C) *MAF* expression levels in Parental cells transduced with mock, *MAF Short*, *MAF Long* or *MAF Short* and *Long* spliced isoform expressing viral particles (Left) and in BoM2 shControl, shMAF or Rescue BoM2 cells (Right). *MAF long* expression levels were determined by qRT-PCR using TaqMan probe and normalized to *B2M* levels. *MAF short* endogenous levels were determined by qRT-PCR using Syber Green reaction with indicated primers and normalized to *b-ACTIN* levels. Presence of ectopically expressed *MAF short* isoform was detected by qRT-PCR using Syber Green reaction with indicated primers described at the material and method section.

D) Up, Western Blot depicting MAF protein levels in Parental mock, MAF Short and MAF Long spliced isoform overexpressing cells (simultaneously) and in BoM2 Control, shMAF or Rescue BoM2 cells. α- TUBULIN was used as loading control. Down, MAF IHC using sections of FFPE cell pellets of the indicated populations. Scale bar, 50 μM.

E) Renilla activity of C-MARE reporter plasmid in Parental cells transiently transfected with mock, *MAF Short*, *MAF Long* or *MAF Short* and *Long* spliced isoform expressing viral particles. Activity of C-MARE promoter was normalized to Control condition and presented in arbitrary units. Data is mean of three independent experiments with S.D.

F) (Left) Tumor growth from Parental mock and MAF Short and MAF Long spliced isoform overexpressing cells (simultaneously) cells injected orthotopically in mouse mammary fat pad was scored. Data are presented as box plot with median, IQR and min and max values. (Right) Percentage of Ki67-positive cells in mammary fat pad tumors from Parental mock or *MAF Short and MAF Long* isoform overexpressing cells (simultaneously). For each tumor a minimum of 10

random fields were counted for Ki67-positive cells. Values are mean with S.D. (n=4). P-value scored by two-sided Wilcoxon signed-rank test

G) *ex vivo* bioluminescent signal and H&E at hind limbs of mice in each indicated experimental group. Scale bar, 50 μM.

H) (Left) Quantification of *ex vivo* bioluminescent signal at hind limbs of mice in each indicated experimental group. Black line depicts average intensity. (Right) Representative bioluminescent images of *ex vivo* hind limbs at endpoint, day 54, and H&E staining of bone metastasis for each group are shown. Tumor area-black dashed line. P-value scored by two-sided Wilcoxon signed-rank test

I) (Left) Quantification of *ex vivo* bioluminescent signal at hind limbs of mice in each indicated experimental group. Data are presented as box plot with median, IQR and min and max values. (Right) Representative bioluminescent images of *ex vivo* hind limbs at endpoint, day 54, with representative CT scans and representative H&E staining of bone metastasis for each group are shown. Scale bars, 500 and 50 μm for the middle and right panel respectively. Tumor area-black dashed line. Histomorphometric analysis of bone metastasis lesions is depicted (BV/TV, Bone Area, Tumor Area). P-values scored by two-sided Wilcoxon signed-rank test. *<0.05.

J) (Left), Quantification of *ex vivo* bioluminescent signal at hind limbs of mice injected via left ventricle with Parental mock or MAF Short or Long spliced isoform expressing cells. (Right), Representative bioluminescent images at day 0 and at endpoint, day 54, representative H&E staining of bone metastatic lesions at end point for each group are shown. Scale bar, 500 μm. P-value scored by two-sided Wilcoxon signed-rank test

K) Incidence of adrenal (Left) and lung (Right) metastasis in mice injected with Parental mock and *MAF Short* and *Long* isoform overexpressing cells (simultaneously) via left ventricle in 3D. P-value scored by two-sided Wilcoxon signed-rank test

L) Kaplan-Meier curve of lung metastasis-free survival for Parental mock, *MAF Short* and *Long* isoform overexpressing (simultaneously) and MDA231-LM2 cells after tail vein injection. P-value scored by two-sided Wilcoxon signed-rank test

M) Histomorphometric analysis of bone metastasis lesions from the indicated groups is depicted (Osteoclast number/ Tumor-Bone interface, BV/TV, Bone Area, Tumor Area). P-values scored by two-sided t test. *<0.05.

N) Incidence of soft tissue metastasis of mice injected with T47D mock and *MAF Short* and *Long* isoform overexpressing (simultaneously) cells via left ventricle in main Figure 3E. P-value scored by two-sided Wilcoxon signed-rank test.

O) Kaplan-Meier curve of lung metastasis-free survival for T47D mock and *MAF Short* and *Long* isoform overexpressing (simultaneously) cells after tail vein injection.

P) Quantification of *in vivo* bioluminescent intra tibiae injected Parental Mock and MAF overexpressing 4T1 cells in mice in each indicated experimental group. Data are presented as box plot with median, IQR and min and max values. Wilcoxon signed-rank test was used.

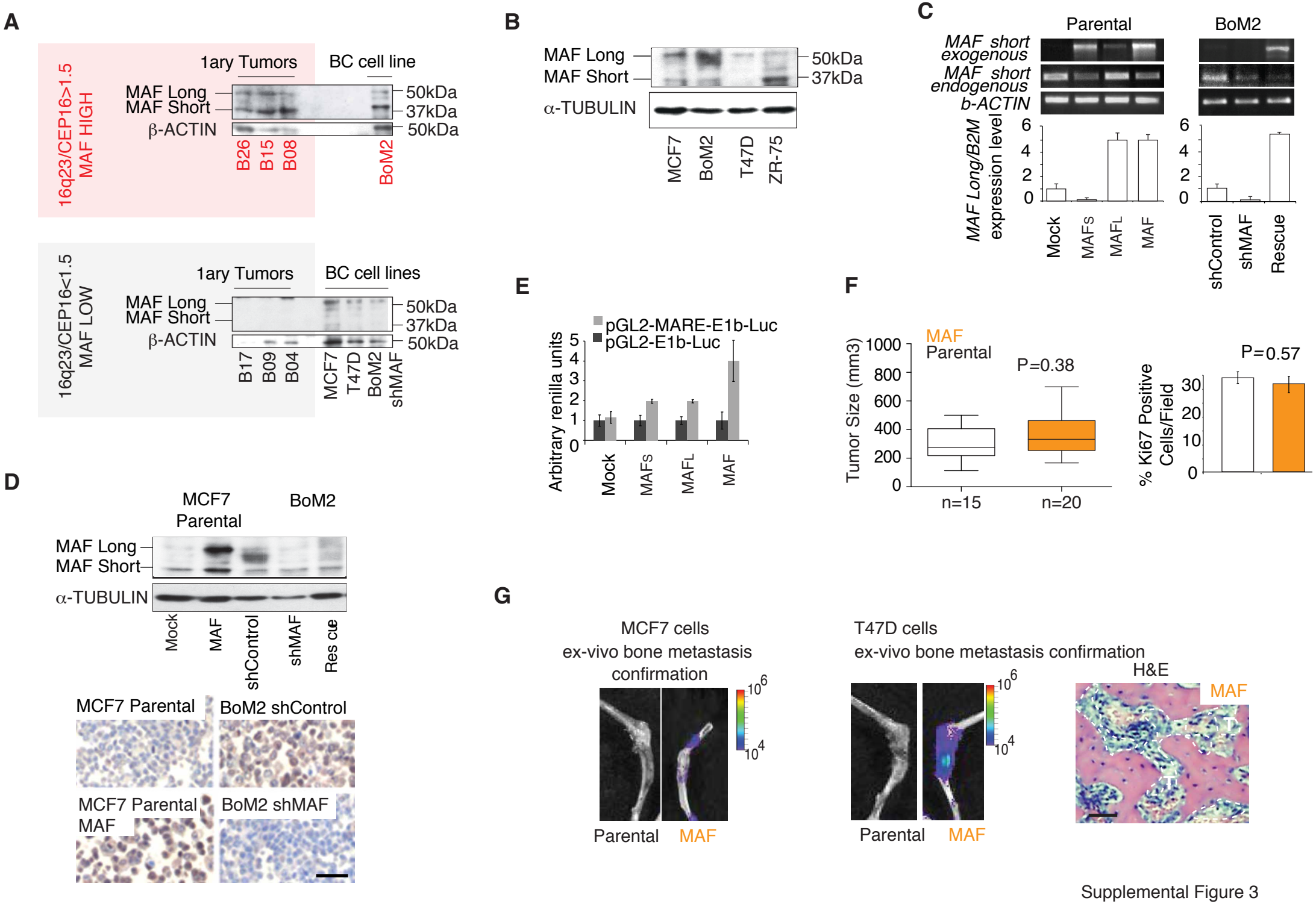

Supplemental Figure 3

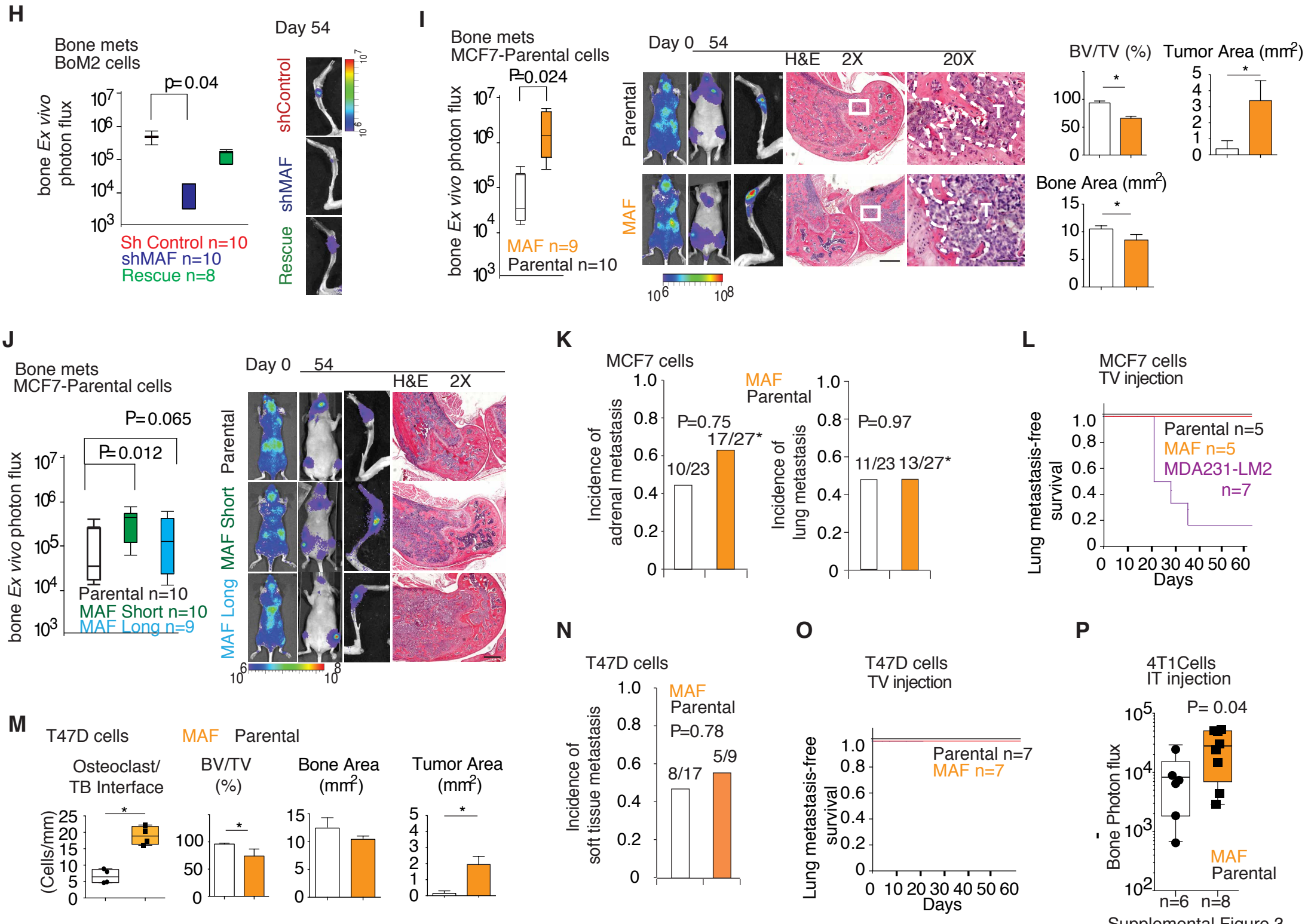

Supplemental Figure 3

Supplementary Figure 4

A) Gene list represents genes comprising MAF long and short metastasis program defined in MCF7 Parental cell line. Green and red box depict MAF Short and Long down regulated and up regulated genes, respectively. Genes described to be involved in different physiological processes are color-coded.

B) Quantification of wound closure assay. The percentage of closure after 48 hours was calculated for each experimental group. Data is mean of three experiments with S.D. Wilcoxon signed-rank test was used.

C) Osteoclast differentiation assay *in vitro*. Bone marrow monocyte cells were differentiated to osteoclast for 7 days in presence of RANKL and MCSF and conditional media from indicated tumor cells, as described in method section. Quantification of the number of TRAP+ differentiated multinucleated (>3 nuclei) osteoclast per field, normalized to control, is presented for indicated experimental conditions. Data is mean of three experiments with S.D. P-value scored by two-sided Wilcoxon signed-rank test.

A

MAFshort and long metastasis program

	entrez	symbol
MAF$_{SL}$ Down Regulated	79719	AAGAB
	54796	BNC2
	1411	CRYBA1
	29909	GPR171
	23493	HEY2
	26155	NOC2L
	5376	PMP22
	860	RUNX2
	6659	SOX4
	7035	TFPI
	22834	ZNF652
MAF$_{SL}$ Up Regulated	9429	ABCG2
	655	BMP7
	948	CD36
	956	ENTPD3
	8817	FGF18
	2669	GEM
	3486	IGFBP3
	3693	ITGB5
	3860	KRT13
	3866	KRT15
	131578	LRRC15
	4133	MAP2
	5744	PTHLH
	6414	SEPP1
	7456	WIPF1
	678	ZFP36L2

Bone Remodelling
Survival/Proliferation
Differentiation
Migration/adhesion
RNA Processing
Cell signaling
Stress/Metabolism

B

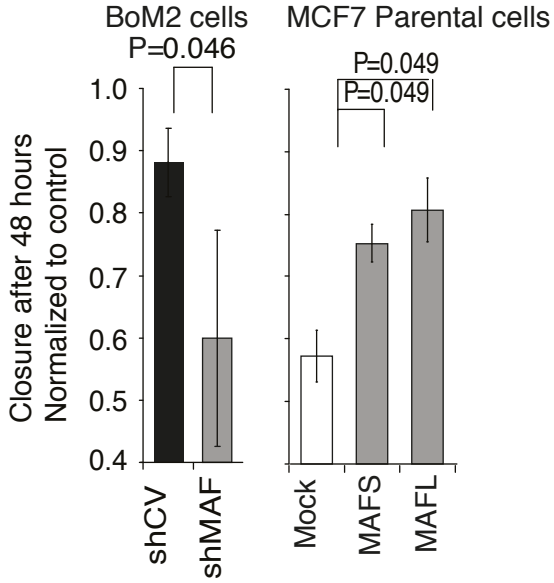

C

In vitro osteoclast differentiation assay

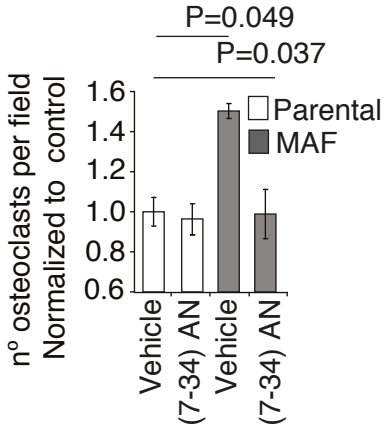

Supplemental Figure 4

Supplementary Figure 5

A) Expression levels of *PTHrP* in Parental mock, *MAF Short* and *Long* spliced isoform overexpressing cells (independently or collectively) measured by qRT-PCR using TaqMan probe genes and normalized to *B2M* levels. n.d. below detection limits. Data is mean of three experiments with S.D

B) Expression levels of *PTHrP* in Parental mock, *MAF Short* and *Long* spliced isoform (simultaneously) and *MAF Short* and *Long* isoform shPTHrP cells measured by qRT-PCR using TaqMan probe genes and normalized to *B2M* levels. Data is mean of three experiments with S.D

C) Incidence of lung (Left) and adrenal (Right) metastasis in mice injected with Parental *MAF* Short and Long isoform overexpressing (simultaneously) and *MAF* Short and Long isoform overexpressing (simultaneously) shPTHrP cells via left ventricle in main Figure 6A. P-value scored by two-sided Wilcoxon signed-rank test.

D) Incidence of lung (Left) and adrenal (Right) metastasis in mice injected with BoM2 shControl and shPTHrP cells in 6B.

E) Incidence of lung (Left) and adrenal (Right) metastasis in mice injected with *MAF* Short and Long isoform overexpressing (simultaneously) MCF7 cells treated with or without PTHrP-AN peptide (7-34 AN) in 6D.

F) Representative TRAP staining of bone metastasis for mice injected with Parental MCF7 cells treated with placebo or PTHrP antagonist in main Figure 6D. Scale bar, 100 μM.

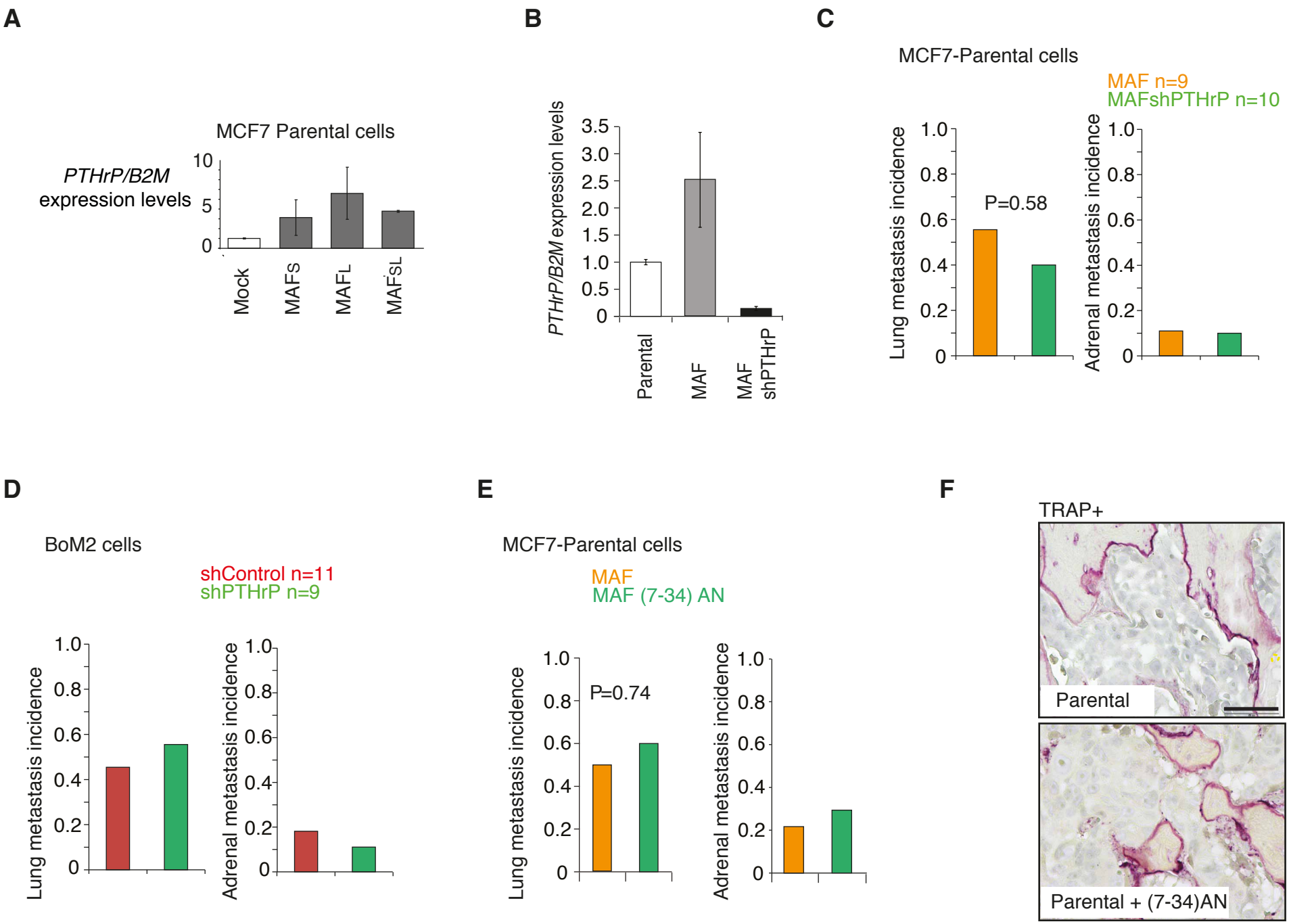

Supplemental Figure 5